Single Delivery of an Adeno-Associated Viral Construct to Transfer the *CASQ2* Gene to Knock-In Mice Affected by Catecholaminergic Polymorphic Ventricular Tachycardia Is Able to Cure the Disease From Birth to Advanced Age

Marco Denegri, PhD*; Rossana Bongianino, MSc*; Francesco Lodola, PhD*; Simona Boncompagni, PhD; Verónica C. De Giusti, MD, PhD; José E. Avelino-Cruz, PhD; Nian Liu, MD; Simone Persampieri, MS; Antonio Curcio, MD, PhD; Francesca Esposito, MD; Laura Pietrangelo, MSc; Isabelle Marty, PhD; Laura Villani, MD; Alejandro Moyaho, PhD; Paola Baiardi, PhD; Alberto Auricchio, MD; Feliciano Protasi, PhD; Carlo Napolitano, MD, PhD; Silvia G. Priori, MD, PhD

Background—Catecholaminergic polymorphic ventricular tachycardia is an inherited arrhythmogenic disorder characterized by sudden cardiac death in children. Drug therapy is still insufficient to provide full protection against cardiac arrest, and the use of implantable defibrillators in the pediatric population is limited by side effects. There is therefore a need to explore the curative potential of gene therapy for this disease. We investigated the efficacy and durability of viral gene transfer of the *calsequestrin 2* (*CASQ2)* wild-type gene in a catecholaminergic polymorphic ventricular tachycardia knock-in mouse model carrying the $CASQ2^{R33Q/R33Q}$ (R33Q) mutation.

Methods and Results—We engineered an adeno-associated viral vector serotype 9 (AAV9) containing cDNA of *CASQ2* wild-type (AAV9-*CASQ2*) plus the *green fluorescent protein* (*GFP*) gene to infect newborn R33Q mice studied by in vivo and in vitro protocols at 6, 9, and 12 months to investigate the ability of the infection to prevent the disease and adult R33Q mice studied after 2 months to assess whether the AAV9-*CASQ2* delivery could revert the catecholaminergic polymorphic ventricular tachycardia phenotype. In both protocols, we observed the restoration of physiological expression and interaction of CASQ2, junctin, and triadin; the rescue of electrophysiological and ultrastructural abnormalities in calcium release units present in R33Q mice; and the lack of life-threatening arrhythmias.

Conclusions—Our data demonstrate that viral gene transfer of wild-type *CASQ2* into the heart of R33Q mice prevents and reverts severe manifestations of catecholaminergic polymorphic ventricular tachycardia and that this curative effect lasts for 1 year after a single injection of the vector, thus posing the rationale for the design of a clinical trial. **(*Circulation*. 2014;129:2673-2681.)**

Key Words: arrhythmias, cardiac ■ calsequestrin ■ death, sudden ■ genetic therapy ■ recovery of function

Catecholaminergic polymorphic ventricular tachycardia (CPVT) is a life-threatening familial disorder characterized by adrenergically mediated arrhythmias in a structurally normal heart that may lead to sudden death.[1] Two genetic forms of CPVT have been identified: the autosomal-dominant variant caused by mutations in the *cardiac ryanodine receptor type 2* (*RyR2)* gene[2] and the autosomal-recessive variant

Editorial see p 2633
Clinical Perspective on p 2681

Received October 16, 2013; accepted April 11, 2014.

From Molecular Cardiology, IRCCS Fondazione Salvatore Maugeri, Pavia, Italy (M.D., R.B., F.L., V.C.D.G., J.E.A.-C., S.P., A.C., F.E., P.B., C.N., S.G.P.); CeSI-Center for Research on Ageing & DNI-Department of Neuroscience and Imaging, University G. d'Annunzio, Chieti, Italy (S.B., L.P., F.P.); Facultad de Ciencias Médicas, Centro de Investigaciones Cardiovasculares, UNLP-CONICET, La Plata, Argentina (V.C.D.G.); Laboratorio de Cardiología Molecular, Insituto de Fisiología, Benemérita Universidad Autónoma de Puebla, Puebla, México (J.E.A.-C.); Department of Cardiology, Beijing Anzhen Hospital, Capital Medical University, Beijing, China (N.L.); Division of Cardiology, Department of Medical and Surgical Science, University of "Magna Graecia," Catanzaro, Italy (A.C.); Federico II University of Naples, Cardiology, Naples, Italy (F.E.); INSERM U836, Grenoble Institut des Neurosciences, Equipe Muscle et Pathologies, Grenoble, France (I.M.); Université Joseph Fourier, Grenoble, France (I.M.); Pathology Division, IRCCS Fondazione Salvatore Maugeri, Pavia, Italy (L.V.); Laboratorio de Ecología de la Conducta, Instituto de Fisiología, Benemérita Universidad Autónoma de Puebla, Puebla, México (A.M.); Telethon Institute of Genetics and Medicine, Naples, Italy (A.A.); Medical Genetics, Department of Translational Medicine, "Federico II" University, Naples, Italy (A.A.); and Department of Molecular Medicine, University of Pavia, Pavia, Italy (S.G.P.).

*Dr Denegri, R. Bongianino, and Dr Lodola contributed equally.

The online-only Data Supplement is available with this article at http://circ.ahajournals.org/lookup/suppl/doi:10.1161/CIRCULATIONAHA.113.006901/-/DC1.

Correspondence to Silvia G. Priori, MD, PhD, Division of Cardiology and Molecular Cardiology, Maugeri Foundation–University of Pavia, Via Maugeri 10/10°, 27100, Pavia, Italy. E-mail silvia.priori@fsm.it

caused by mutations in the *cardiac calsequestrin 2* (*CASQ2*) gene.[3] Additionally, 4 other genes have been associated with a clinical spectrum of manifestations consistent with the diagnosis of CPVT or with its phenocopies.[4–6]

Interestingly, *RyR2* and *CASQ2* mutations induce diastolic Ca^{2+} release from the sarcoplasmic reticulum (SR), leading to the development of delayed afterdepolarizations (DADs) and triggered activity (TA), which may precipitate life-threatening arrhythmias.[7–10] This arrhythmogenic mechanism has been confirmed in patients during monophasic action potential recordings that documented the presence of adrenergically mediated DADs and TA in patients with CPVT.[11]

CPVT, unless promptly diagnosed and treated, may be lethal, as documented by the fact that up to 30% of untreated individuals die suddenly before the fourth decade of life.[12,13] Clinical management of CPVT is based on treatment with β-blockers, which attenuate the consequences of adrenergic stimulation, often combined with the sodium channel blocker flecainide,[14–16] which may directly inhibit TA. Patients unresponsive to this therapy are candidates for implantation of a cardioverter-defibrillator,[16] which is a most valuable life-saving therapy but presents a high rate of complications in the pediatric population.[17] Because the recurrence of life-threatening arrhythmic episodes on medications is quite common in patients with CPVT despite compliance with β-blocker therapy (25% recurrences in our unpublished data and 27% in the series by Hayashi et al[12]), there is a need for new therapeutic approaches and for the identification of a cure for this disease.

We have recently initiated a set of studies aimed at the development of a curative treatment for the recessive form of CPVT. In our first published study,[18] we demonstrated the feasibility of intraperitoneal *CASQ2* gene delivery using an adeno-associated viral vector (AAV9) in *CASQ2* knockout newborn mice. The study proved the ability of this approach to preserve physiological levels of calsequestrin 2 (CASQ2) and its related proteins, triadin and junctin, in the heart of *CASQ2* knockout mice, and it showed that overexpressed CASQ2 localizes properly in the heart of mice and is able to prevent DADs, TA, and the development of life-threatening arrhythmias.[18]

Despite these encouraging results, it is clear that the development of a curative strategy for CPVT applicable in the clinical setting should prove that (1) the efficacy and lack of side effects of viral gene transfer are documented not only in a knockout animal model but, most important, in a knock-in model of the human disease, (2) there is evidence for long-term maintenance of the antiarrhythmic response, and (3) the treatment is able to prevent the disease when administered in neonates and to revert all the phenotypic manifestations when therapy is administered in adults.

Accordingly, in the present study, we investigated whether the in vivo delivery of the AAV9-*CASQ2* construct to homozygous knock-in *CASQ2*$^{R33Q/R33Q}$ (R33Q) mice would meet those criteria. Our study was therefore targeted to investigate the ability of AAV9-*CASQ2* to prevent the development of CPVT in R33Q mice infected at birth, to verify the efficacy of the viral gene transfer to prevent the onset of the disease after a medium and long period after a single infection delivered at birth, and to assess the ability of AAV9-*CASQ2* gene delivery to revert the disease when administered to adult R33Q mice with an overt CPVT phenotype.

Methods

A more detailed description of methods is provided in the online-only Data Supplement.

Viral Construct

In the present study, we used an AAV9 carrying the complete cDNA of the murine cardiac *CASQ2* cotranscribed, through an internal ribosome entry site sequence, with the *green fluorescent protein* (*GFP*) gene as previously described.[18]

Generation of R33Q Knock-In Mouse Model

A homozygous R33Q knock-in strain was previously generated in our laboratory.[10] Animals were bred and raised at the Charles River Laboratories (Calco, Italy) and transferred to the animal facility at the Maugeri Foundation for phenotypic characterization.

AAV9-*CASQ2* Infection Procedure in R33Q Mice

The AAV recombinant virus (AAV9-*CASQ2*) and the empty virus (AAV9-*GFP)* were produced by the AAV Vector Core of the Telethon Institute of Genetics and Medicine (Napoli, Italy) according to a previously published protocol.[18] The viral titer was 2.6×10^{12} genome copies per milliliter for AAV9-*CASQ2* and 4.3×10^{12} genome copies per milliliter for AAV9-*GFP*. The infection was performed by intraperitoneal injection in pups on postnatal day 3 (100 μL), which recovered until euthanasia was performed at 6, 9, or 12 months. Three-month-old mice were anesthetized with Avertin (0.025 mg/kg), and viral particles (200 μL) were injected into the tail vein and studied 2 months later. ECG recordings in mice of either sex were performed with implantable loop recorders (Data Sciences International).

In Vitro Electrophysiology

Ventricular myocytes were enzymatically dissociated through aortic retrograde perfusion. Action potentials were recorded by use of the

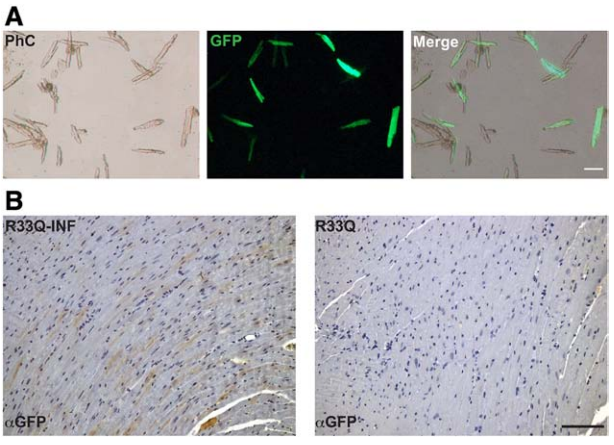

Figure 1. Long-term postinfection analysis of the efficiency and distribution of the green fluorescent protein (GFP)–tagged AAV9-*CASQ2* construct delivered to newborn R33Q mice. **A**, Estimation of infection rate (40%–50%, as evidenced by the merge) of infected GFP-positive cells compared with total cells (phase contrast [PhC]). Scale bar, 100 μm; n=3 mice for each age. **B**, Immunohistochemistry analysis with an anti-GFP antibody (dark brown) counterstained with hematoxylin (blue) to highlight the tissue distribution of AAV9-*CASQ2* infection after 12 months in R33Q-INF. R33Q was used as the negative control. Scale bar, 100 μm; n=3 mice.

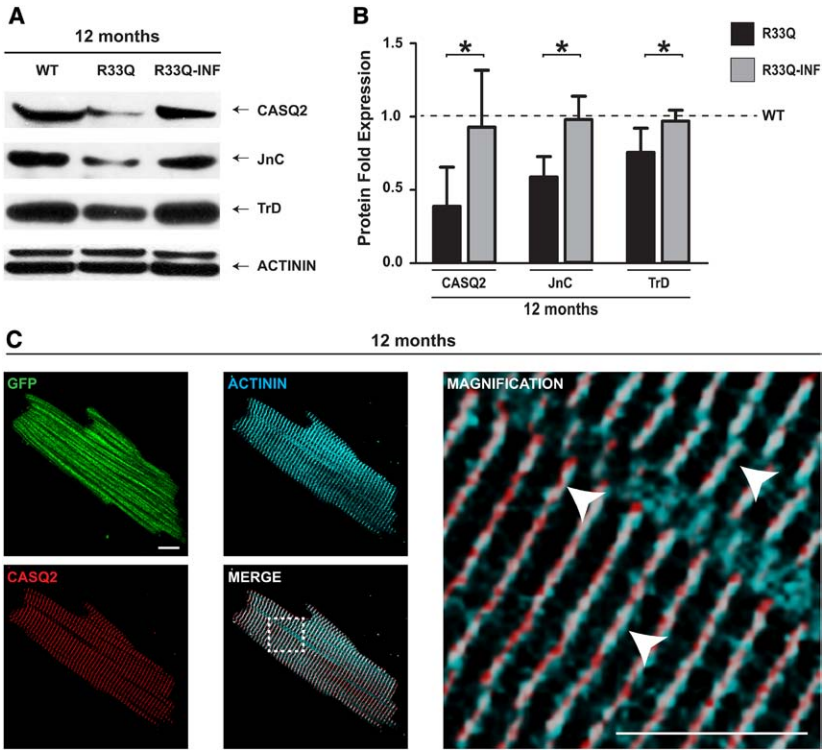

Figure 2. Long-term postinfection analysis of protein expression and localization in AAV9-*CASQ2* infected newborn R33Q mice. **A**, Protein expression analysis of CASQ2, junctin (JnC), and triadin (TrD) in wild-type (WT), R33Q, and AAV9-*CASQ2*–infected newborn R33Q (R33Q-INF) mice 12 months after infection. **B**, Protein quantification of CASQ2, JnC, and TrD in hearts derived from WT, R33Q, and R33Q-INF mice at 12 months (n=3 mice for each condition). Data are normalized to WT levels±SD (*P<0.05). **C**,Distribution of the overexpressed CASQ2 protein in an infected green fluorescent protein (GFP)–positive myocyte 12 months after AAV9-*CASQ2* delivery. CASQ2 is colocalizing with α-actinin along the z lines (magnification, white arrowheads). Scale bars, 10 μm.

whole-cell patch clamp technique in the current-clamp mode and analyzed with pCLAMP 9.2 (Molecular Devices).

Reverse-Transcription Polymerase Chain Reaction and Quantitative Real-Time Polymerase Chain Reaction

Total RNA was extracted and purified from isolated myocytes, liver, lung, skeletal muscle, spleen, kidney, testis, and ovary of AAV9-*CASQ2*–infected R33Q and R33Q mice. Real-time polymerase chain reaction quantification of mRNA was processed and analyzed as previously described.[18]

Immunoblotting

Protein expression analysis was performed with the following antibodies: anti-CASQ2 (ABR), anti-triadin,[6] anti-junctin,[18] anti-RyR2 (ABR), anti–α-actinin (Sigma-Aldrich), and anti-cadherin (Sigma-Aldrich).

Immunoprecipitation

Protein-protein interaction was studied by coimmunoprecipitation with anti-triadin antibody.[6] AAV9-*CASQ2*–infected R33Q and R33Q hearts were washed with PBS and lysed in the presence of protease inhibitors according to the manufacturer's instructions (Dynabeads Coimmunoprecipitation Kit, Invitrogen). An unrelated anti-rabbit IgG (Promega) was used as negative control.

Immunohistochemistry

Hearts were collected and processed for paraffin embedding. The sections were incubated with hematoxylin and eosin and Masson trichrome staining. Immunohistochemical analysis was performed with an anti-GFP antibody (Santa Cruz).

Confocal Microscopy

Indirect immunofluorescent labeling of cardiac myocytes isolated from AAV9-*CASQ2*–infected R33Q mice was performed as previously described.[18]

Electron Microscopy

Fixed hearts of either sex were embedded in an epoxy resin, and ultrathin sections were cut, stained, and analyzed as previously described.[10]

Statistics

Data are reported as mean±SEM unless otherwise specified. Continuous variables were analyzed by the unpaired *t* test. Categorical variables were analyzed by contingency tables with the Fisher exact test. We used generalized linear mixed models with a binomial

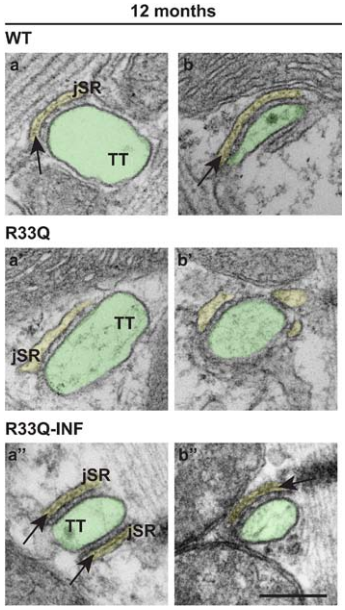

Figure 3. Ultrastructural analysis of calcium release units (CRUs) in 12-month-old wild-type (WT), R33Q, and R33Q mice infected with AAV9-*CASQ2* at birth. Electron micrographs of junctions between transverse tubules (TTs) and junctional sarcoplasmic reticulum (jSR; ie, CRUs) from WT (**a** and **b**), R33Q (**a′** and **b′**), and AAV9-*CASQ2*–infected newborn R33Q (R33Q-INF; **a′′** and **b′′**) hearts 12 months after infection (n=3 mice for each condition). TTs are labeled in green; JSR is in yellow. Black arrows point to the electron-dense polymer of CASQ2 inside the jSR lumen. Scale bar, 0.1 μm.

structure of the errors and a logit link function to investigate whether there is a relationship between the responses (DADs and TA) and the explanatory variable (the genetic group: wild type [WT], R33Q, R33Q-INF, R33Q-GFP). Accordingly, DADs and TA were scored as present (1) or absent (0) in the mice. Cells, mice, and time since infection were random-effect variables, and genetic group was the explanatory variable. Model simplification was also used to obtain minimal adequate models.[19] We used the likelihood ratio test for model selection, Wald z test for comparing 2 factor levels, and Dunnett contrasts for multiple comparisons. All statistical analyses were carried out with R software. Values of $P<0.05$ were considered statistically significant.

Results

Results are presented for 2 sets of experiments. The data in the first sections are related to the protocol designed to test whether a single injection of the AAV9-*CASQ2* delivered at birth in R33Q mice is able to prevent the development of CPVT up to 1 year of age corresponding to advanced age for mice. The second set of data relate to the protocol designed to test whether a single injection of the AAV9-*CASQ2* construct in adult R33Q mice is able to revert phenotypic manifestations of CPVT.

Efficacy and Long-Term Persistence of the Effects of a Single Injection of AAV9-CASQ2 at Birth in R33Q Mice

We studied 3 groups of mice at different times (6, 9, and 12 months) after injection to characterize the effect of therapy on (1) efficiency of infection; (2) levels of CASQ2 and its associated proteins, triadin and junctin; (3) architecture of calcium release units (CRUs); (4) in vitro response of R33Q myocytes to isoproterenol; and (5) adrenergically mediated arrhythmogenesis in vivo.

Efficiency of AAV9-CASQ2 Infection

We quantified the infection rate by epifluorescent analysis in isolated ventricular cardiomyocytes in R33Q mice infected at birth with AAV9-*CASQ2* (R33Q-INF). We observed an infection rate between 40% and 50% (Figure 1A). As depicted in Figure 1B, the viral distribution, detected by a specific anti-GFP immunohistochemistry, revealed a mosaic expression into cardiac tissues. *GFP* expression was quantified by real-time polymerase chain reaction in different organs. As expected for AAV9,[20–22] cardiac myocytes were the main target of the viral infection (Figure IA in the online-only Data Supplement). Histological analysis did not reveal structural abnormalities or inflammation in infected hearts at 12 months (Figure IB in the online-only Data Supplement).

Levels of CASQ2 and Its Associated Proteins, Triadin and Junctin

The cardiac mRNA expression analysis by real-time polymerase chain reaction of *CASQ2* did not evidence significant changes in the endogenous transcript in R33Q and R33Q-INF mice (Figure IIA in the online-only Data Supplement). Comparison between endogenous and total transcript in R33Q-INF mice provided evidence of the increase in *CASQ2*-mRNA caused by the AAV9 infection (Figure IIB in the online-only Data Supplement). Furthermore, the protein analysis in R33Q and R33Q-INF mice allowed us to point out the increased level of AAV-induced CASQ2 (Figure IIC and IID in the online-only Data Supplement). The expression of CASQ2 and its ancillary partners, junctin and triadin, in $CASQ2^{WT/WT}$ (WT), R33Q, and R33Q-INF mice was analyzed 12 months after viral infection. In agreement with our previous report,[10] we documented that the homozygous R33Q mice present a major reduction in levels of CASQ2, junctin, and triadin as assessed by Western blot analysis (−62% in CASQ2, −42% in junctin, and −24% in triadin at 12 months; Figure 2A and 2B). In the R33Q-INF animals, however, there was a significant recovery of the levels of the 3 proteins (Figure 2A and 2B). We assessed the cellular distribution of the virally induced CASQ2, showing that it correctly localized along the z lines (Figure 2C). A comparison of CASQ2 expression between R33Q and R33Q-INF myocytes is shown in Figure III in the online-only Data Supplement.

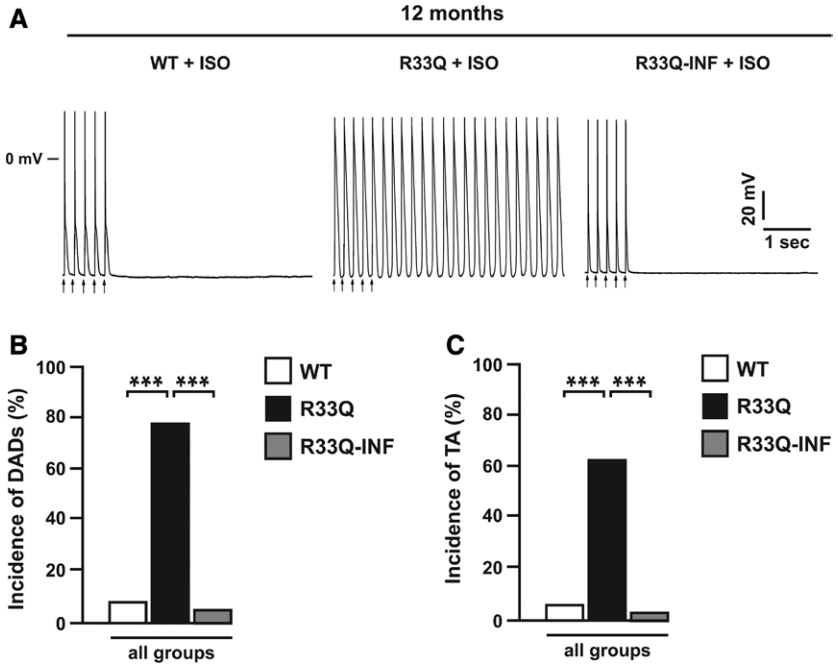

Figure 4. In vitro electrophysiological analysis after AAV9-*CASQ2* infection in newborn R33Q mice. **A**, Action potentials elicited at 5 Hz (arrows) after exposure to 30 nmol/L isoproterenol (ISO) in isolated myocytes from wild-type (WT), R33Q, and AAV9-*CASQ2*–infected R33Q (R33Q-INF) mice at 12 months. Quantification of the incidence of (**B**) isoproterenol-induced delayed afterdepolarizations (DADs; defined as phase 4 positive transient depolarizing deflections of the membrane potentials) and (**C**) triggered activity (TA; defined as an unstimulated action potential developing from a DAD) in all groups of WT, R33Q, and R33Q-INF myocytes: $DADs_{WT}$, 5 of 60 cells; $DADs_{R33Q}$, 47 of 61 cells; $DADs_{R33Q\text{-}INF}$, 3 of 54 cells; TA_{WT}, 3 of 60 cells; TA_{R33Q}, 38 of 61 cells; and $TA_{R33Q\text{-}INF}$, 1 of 54 cells. ***$P<0.001$, R33Q-INF vs R33Q and WT vs R33Q (n=3 mice for each condition).

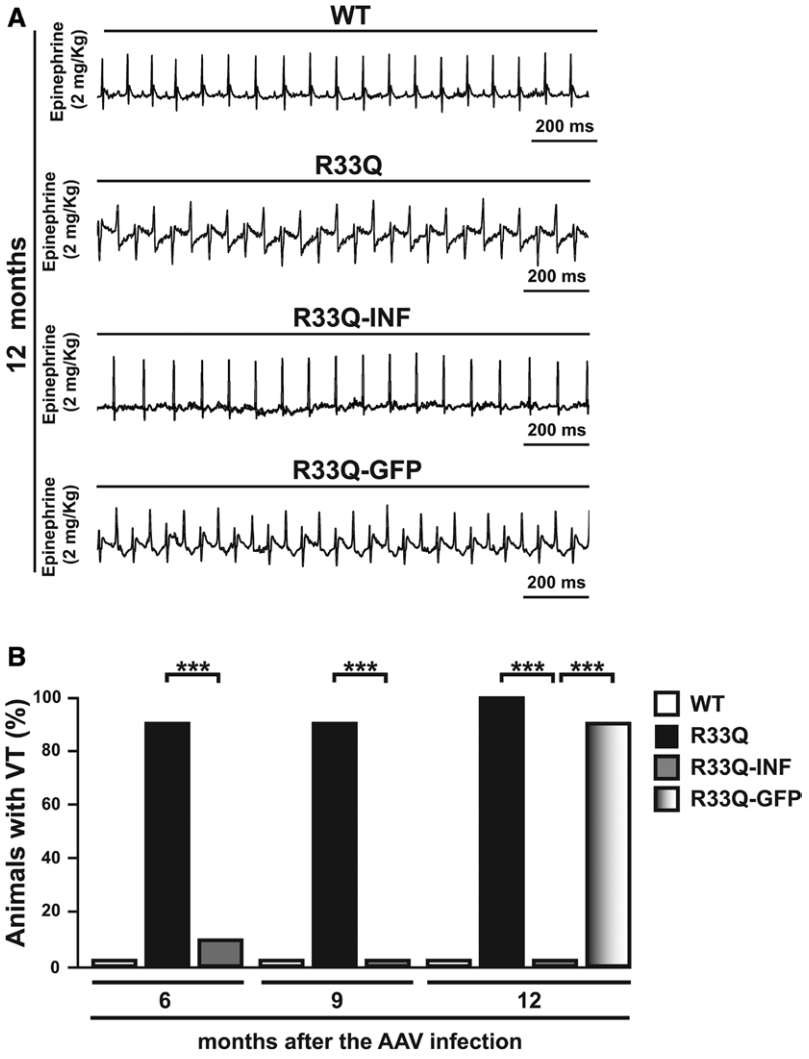

Figure 5. In vivo ECG recording after medium- and long-term AAV9-*CASQ2* infection in newborn R33Q mice. **A**, In vivo epinephrine administration elicited bidirectional ventricular tachycardia in R33Q and R33Q-GFP, but not in WT or AAV9-*CASQ2*–infected, newborn R33Q (R33Q-INF) mice. **B**, Quantification of the incidence of ventricular tachycardia (VT) in WT, R33Q, R33Q-INF, and R33Q-GFP mice after 6, 9, and 12 months ($VT_{WT\text{-}6\ months}$, 0 of 9 mice; $VT_{WT\text{-}9\ months}$, 0 of 9 mice; $VT_{WT\text{-}12\ months}$, 0 of 6 mice; $VT_{R33Q\text{-}6\ months}$, 8 of 9 mice; $VT_{R33Q\text{-}9\ months}$, 9 of 10 mice; $VT_{R33Q\text{-}12\ months}$, 8 of 8 mice; $VT_{R33Q\text{-}INF\text{-}6\ months}$, 1 of 10 mice; $VT_{R33Q\text{-}INF\text{-}9\ months}$, 0 of 8 mice; $VT_{R33Q\text{-}INF\text{-}12\ months}$, 0 of 8 mice; and $VT_{R33Q\text{-}GFP\text{-}12\ months}$, 7 of 8 mice. ***$P$<0.001, R33Q-INF vs R33Q and R33Q-INF vs R33Q-GFP.

Architecture of CRUs

We recently reported the presence of ultrastructural abnormalities in R33Q mice characterized by widening of the cisternae of junctional SR (jSR) and fragmentation and heterogeneity of couplons.[10,18,23] Furthermore, we observed an absence of the electron-dense CASQ2 polymer in the jSR cisternae.

Here, we show that infection with AVV9-*CASQ2* in neonate R33Q mice prevents the development of abnormal jSR and avoids the loss of CASQ2 polymers and the enlargement of jSR cisternae (jSR width, 33±8 nm in R33Q, 24±7 nm in R33Q-INF; P<0.001; Figure 3). Interestingly, in mice infected with an empty AAV9 vector (R33Q-GFP), there was no rescue of the abnormal CRUs (jSR width in R33Q-GFP, 36±11 nm; Figure IV in the online-only Data Supplement).

Electrophysiological Response of R33Q Myocytes to Isoproterenol

Action potentials of paced (5 Hz) ventricular myocytes derived from WT, R33Q, and R33Q-INF mice infected at birth were recorded by patch-clamp technique to assess the arrhythmogenic response to β-adrenergic stimulation (isoproterenol 30 nmol/L) at different ages (6, 9, and 12 months). The AAV9-*CASQ2* delivery achieved a striking reduction in isoproterenol-induced DADs and TA, preventing the development of the arrhythmogenic phenotype observed in myocytes isolated from R33Q mice (P<0.001, R33Q-INF versus R33Q; Figure 4).

Adrenergically Mediated Arrhythmogenesis In Vivo

WT, R33Q and R33Q-INF mice were instrumented with an implantable ECG recorder to compare the incidence of arrhythmias after adrenergic stimulation (epinephrine 2 mg/kg) at 6, 9, and 12 months after virally mediated AAV9-*CASQ2* delivery. As shown in Figure 5A and 5B, R33Q mice presented a remarkable incidence of polymorphic and bidirectional ventricular tachycardia, whereas R33Q-INF mice showed a highly significant suppression of the arrhythmic events (P<0.001, R33Q-INF versus R33Q and R33Q-INF versus R33Q-GFP).

Ability of a Single Infection With the AAV9-CASQ2 Construct to Revert the CPVT Phenotype in Adult Symptomatic R33Q Mice

Three-month-old R33Q mice were instrumented with ECG telemetry to test for arrhythmia susceptibility after administration of epinephrine. Mice that developed either polymorphic or bidirectional ventricular tachycardia were randomized into 2 groups based on the response to this initial test: R33Q mice receiving no viral gene transfer (n=9) and R33Q mice infected

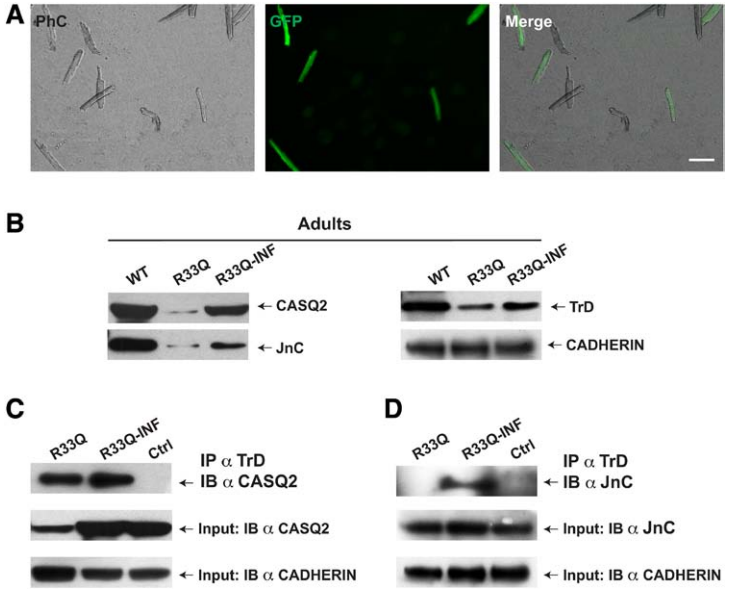

Figure 6. Molecular characterization of AAV9-*CASQ2* infection in adult R33Q mice. **A**, Evaluation of the efficiency of AAV9-*CASQ2* infection in adult R33Q mice 2 months after injection. The rate of viral infection was ≈40% (as shown by the merge) according to the number of green-fluorescent protein (GFP)–positive cells vs total myocytes (phase contrast [PhC]; n=4 mice). **B**, Protein expression analysis in wild-type (WT), R33Q, and R33Q AAV9-*CASQ2*–infected (R33Q-INF) mice. Western blots were performed to detect CASQ2, triadin (TrD), and junctin (JnC). Cadherin was used as the loading control (n=3 mice for each condition). **C** and **D**, Coimmunoprecipitations (IP) in R33Q and R33Q-INF hearts with anti-TrD antibody and immunoblotted (IB) with anti-CASQ2 (**C**) and anti-JnC (**D**) antibody. Cadherin was used as the loading control. An infected heart incubated with unrelated antibody was used as the negative control (Ctrl).

with either AAV9-*CASQ2* (n=13) or AAV9-*GFP* (empty vector; n=3). Two months after the infection, we re-exposed them to ECG challenge and performed molecular, ultrastructural, and electrophysiological assays.

Efficiency of AAV9-CASQ2 Infection

The infection rate was calculated by epifluorescent analysis of GFP expression in isolated cardiac myocytes (Figure 6A). AAV9-*CASQ2* virus delivered in adult mice achieved an infection rate comparable to that of infected newborn mice (≈40%).

Levels of CASQ2, Triadin, and Junctin

Cardiac mRNA expression analysis of *CASQ2* from R33Q and R33Q-INF mice did not provide evidence of significant changes in the endogenous transcript (Figure VA in the online-only Data Supplement). The comparison between the endogenous and total transcript in R33Q-INF provided evidence of the increase in *CASQ2*-mRNA resulting from the AAV9 infection (Figure VB in the online-only Data Supplement). Furthermore, protein analysis in R33Q and R33Q-INF mice allowed us to point out the increased level of AAV-induced CASQ2 (Figure VC and VD in the online-only Data Supplement). Two months after infection with AAV9-*CASQ2*, a normalization of the levels of expression of CASQ2, triadin, and junctin was observed (Figure 6B). At the same time, coimmunoprecipitation experiments with a specific anti-triadin antibody (Figure 6C and 6D) showed that infected cells preserve and restore the physiological protein-protein interactions between triadin and CASQ2 and between triadin and junctin, respectively.

Architecture of CRUs

We performed electron microscopy on cardiac tissue of R33Q and R33Q-INF mice. As shown in Figure 7A, the AAV9-*CASQ2* infection reverted the abnormal morphology of the jSR typical of R33Q mice, inducing a significant reduction in the width of the jSR in R33Q-INF (from 34±9 nm in R33Q to 24±4 nm in R33Q-INF; $P<0.001$). In R33Q-INF hearts, we observed the simultaneous presence of cells with restored CRUs (likely the infected cells) and cardiomyocytes with an abnormal architecture (possibly noninfected cells; Figure 7B).

Electrophysiological Response of R33Q Myocytes to Isoproterenol

Functional analysis was accomplished by in vitro electrophysiology on isolated cardiomyocytes derived from the hearts of R33Q, R33Q-GFP, and R33Q-INF mice (Figure 8A). The action potential profiles elicited at 5 Hz after β-adrenergic stimulation (isoproterenol 30 nmol/L) revealed a remarkable decrease in the percentage of DADs and TA in R33Q-INF versus R33Q cells ($P<0.007$ for both DADs and TA; Figure 8A and the Table).

Adrenergically Mediated Arrhythmogenesis In Vivo

In vivo evaluation of arrhythmias susceptibility was performed by ECG recordings in R33Q, R33Q-GFP, and R33Q-INF mice 2 months after viral gene transfer treatment. An epinephrine test revealed a remarkable reduction in the occurrence of ventricular tachycardia in R33Q-INF mice compared with R33Q mice ($P<0.001$) and R33Q-GFP mice ($P<0.05$; (Figure 8B and the Table).

In a global evaluation of the consequence of administering a single dose of AAV-*CASQ2* therapy in adult R33Q mice, we observed a complete recovery of all the phenotypic manifestations of the recessive CPVT that were present before treatment.

Discussion

The recessive form of CPVT, associated with different *CASQ2* mutations, shares with the autosomal-dominant form of CPVT the same final pathway of SR Ca^{2+} overload, spontaneous diastolic SR Ca^{2+} release, and Ca^{2+} oscillations after adrenergic stimulation that represent a highly arrhythmogenic situation.[24,25] The complex pathogenesis of *CASQ2*-related CPVT is a remarkable example of how a single gene mutation, which determines primarily drastic instability and a reduction in the mutant protein, triggers a cascade of events resulting in biophysical, proteomic, and ultrastructural abnormalities.[9,10,22] Our group has recently demonstrated that it is possible to correct the CPVT phenotype in *CASQ2* knockout mice by AAV transfer of the *CASQ2* gene.[18] However, to replicate what happens in the human form of the disease, we tested our gene

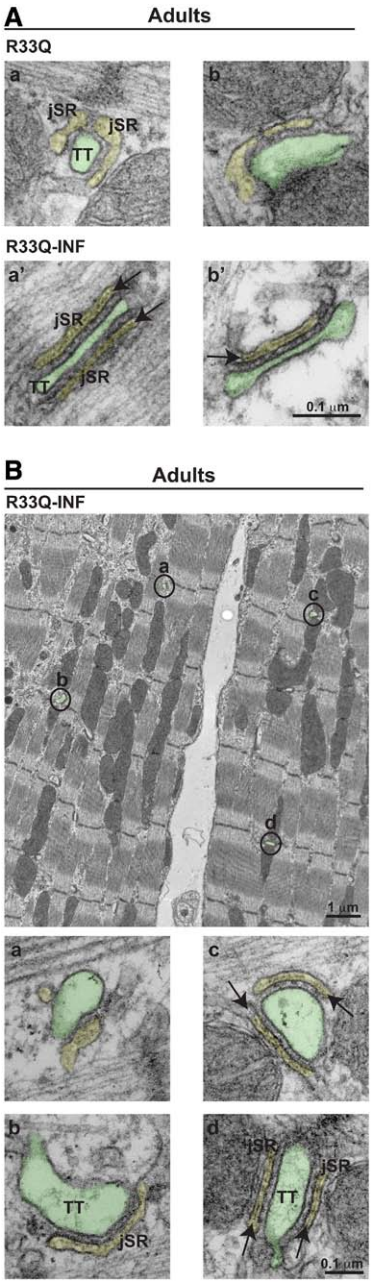

Figure 7. Ultrastructural analysis of the calcium release units (CRUs) in adult R33Q mice infected with AAV9-*CASQ2*. **A**, Electron micrographs of junctions between transverse tubules (TTs) and junctional sarcoplasmic reticulum (jSR; ie, CRUs) from R33Q and AAV9-*CASQ2*–infected adult R33Q (R33Q-INF) hearts (n=3 mice for each condition). TTs are labeled in green; jSR is in yellow. Black arrows point to the electron-dense chain-like polymer of CASQ2 inside the SR lumen. Scale bar, 0.1 μm. **B**, Electron micrograph showing 2 adjacent cardiomyocytes from R33Q-INF mouse. The cell on the **left** contains abnormal CRUs (**a** and **b**). These CRUs present a wide and irregular SR lumen typical of a R33Q cell, whereas the other cardiac cell (**right**) contains structurally restored CRUs (**c** and **d**) with a narrow lumen and chain-like electron CASQ2 polymer. Scale bars, 0.1 and 1 μm.

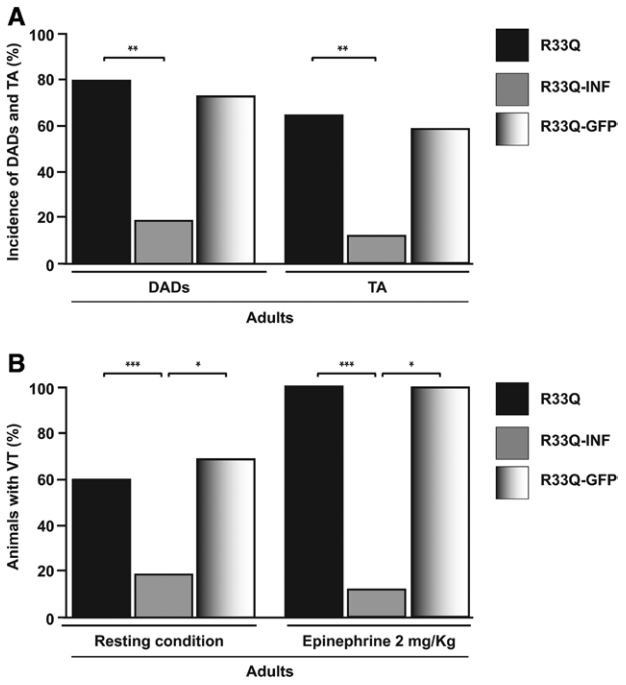

Figure 8. In vitro and in vivo evaluation of susceptibility to arrhythmia in adult R33Q mice after AAV9-*CASQ2* infection. **A**, Incidence of isoproterenol (ISO)-induced delayed afterdepolarizations (DADs) and triggered activity (TA) in infected cardiomyocytes (R33Q-INF) vs control cells (R33Q and R33Q-GFP): $DADs_{R33Q}$, 15 of 19 cells; $DADs_{R33Q\text{-}INF}$, 3 of 17 cells; $DADs_{R33Q\text{-}GFP}$, 9 of 12 cells; TA_{R33Q}, 12 of 19 cells; $TA_{R33Q\text{-}INF}$, 2 of 17 cells; and $TA_{R33Q\text{-}GFP}$, 7 of 12 cells. $^{**}P<0.007$, R33Q-INF vs R33Q (n=3 mice). **B**, Quantification of animals presenting ventricular tachycardia (VT) episodes in the resting condition and after epinephrine administration in adult R33Q (n=9), R33Q-GFP (n=3), and R33Q-INF (n=13) mice. $^{***}P<0.001$, R33Q-INF vs R33Q; $^{*}P<0.05$, R33Q-INF vs R33Q-GFP. GFP indicates green fluorescent protein.

therapy approach in the homozygous R33Q knock-in mouse model, characterized by the expression of an endogenous defective CASQ2 protein.[10] This model is a bigger challenge for the viral gene transfer approach because it is difficult to predict whether the overexpressed wild-type CASQ2 would polymerize with the mutant protein to rescue the composite phenotypic manifestations of the disease.

Data presented in this work prove that a single administration of the viral construct AAV9-*CASQ2* displays long-lasting efficiency in mice infected at birth and is able to revert the phenotype in adult symptomatic mice. These 2 protocols simulate 2 distinct clinical scenarios for the delivery of gene therapy to infants genotyped at birth and to symptomatic individuals diagnosed later in life.

The AAV9-*CASQ2* infection rate in cardiac cells resulted in ≈40% after delivery of the construct in both neonates and adult animals. The functional characterizations combining in vivo and in vitro electrophysiology demonstrated comparable features in AAV infection in newborns and in symptomatic adults, proving that the efficacy of the viral delivery of *CASQ2* is independent of the time of administration of the viral construct. As expected, the virus localized preferentially into the heart, as demonstrated by real-time *GFP* expression and immunohistochemical analysis. The systemic administration of AAV9-*CASQ2* was able to restore the physiological protein levels of CASQ2, triadin, and junctin, providing evidence of their high interdependence and the appropriate localization in the cardiac myocytes.

In addition, coimmunoprecipitation in infected R33Q adult mice suggests that the overexpressed CASQ2 is also

Table. In Vivo and In Vitro Incidence of Arrhythmic Events in Adult R33Q, AAV9-*CASQ2* R33Q, and AAV9-*GFP* R33Q Mice

Mice	In vivo ECG, n mice	VT, % (n mice)	In vitro EP, n cells	DADs, % (n cells)	TA, % (n cells)
R33Q	9	100 (9/9)	19	79 (15/19)	63 (12/19)
R33Q-INF	13	15 (2/13)*‡	GFP(+)=17	18 (3/17)†	12 (2/17)†
			GFP(–)=9	77 (7/9)	66 (6/9)
R33Q-GFP	3	100 (3/3)	GFP(+)=12	75 (9/12)	58 (7/12)
			GFP(–)=5	80 (4/5)	60 (3/5)

The incidence of polymorphic VT (after epinephrine injection 2 mg/kg) and DADs (defined as phase 4 positive transient depolarizing deflections of the membrane potentials) or TA (defined as an unstimulated action potential developing from a DAD) on β-adrenergic stimulation with isoproterenol (30 nmol/L) in R33Q, AAV9-*CASQ2* R33Q (R33Q-INF), and AAV9-*GFP* R33Q (R33Q-GFP) mice 2 months after the viral infection. DAD indicates delayed afterdepolarization; EP, electrophysiology; GFP, green fluorescent protein; and TA, triggered activity.

*$P<0.001$, R33Q-INF vs R33Q.

†$P<0.007$, R33Q-INF vs R33Q.

‡$P<0.05$, R33Q-INF vs R33Q-GFP.

able to retain the physiological protein-protein interaction between triadin and CASQ2 and to restore the molecular binding, missed in R33Q mice, between triadin and junctin. Interestingly, we have shown that our gene therapy strategy is able to recover protein levels and to revert the jSR widening and fragmentation[23] seen in CRUs of R33Q.[10] It is also remarkable that electron microscopy allowed to appreciate the correct localization of the overexpressed CASQ2 in the jSR as documented by the reappearance of the chain-like polymers of CASQ2 in the jSR.[26,27]

A puzzling question raised by our study is why, even though the AAV9-*CASQ2* construct does not reach all cardiac cells, it induces a remarkable antiarrhythmic efficacy. We believe that biophysical properties that regulate the propagation of the action potential in the heart may provide an explanation for this apparently surprising effect. Accordingly, for a triggered action potential to elicit a premature ventricular complex, it has to be able to propagate to adjacent cells. Because action potential propagation follows the "source-sink" relationship, both active and passive properties of the cardiac tissue determine whether an action potential is able to travel from cell to cell. It is only when adjacent myocytes develop synchronous DADs that the summation of the multiple depolarizations allows propagation of a triggered action potential to the entire heart. The experimental demonstration of this concept has been provided in a most elegant in silico study by Xie et al.[28] These authors calculated the number of adjacent cells required for a DAD to generate an action potential and showed that an afterdepolarization is suppressed unless a sufficient number of the neighboring myocytes develop an afterdepolarization on the same beat. Therefore, to prevent propagation of triggered beats, it is not required that all cells are rescued; it is enough that a fraction of them impair propagation of action potentials to prevent life-threatening arrhythmias.

The need for novel and more effective therapies for CPVT and the efficacy observed in our recessive CPVT animal models of *CASQ2* viral gene delivery open the door to gene therapy for CPVT. The recent Calcium Up-Regulation by Percutaneous Administration of Gene in Cardiac Disease (CUPID) study showed the safety and efficacy of AAV-mediated *cardiac delivery of the sarcoplasmic/endoplasmic reticulum Ca^{2+} ATPase 2a* (*SERCA2a*) gene in heart failure patients.[29] These results, combined with the first marketing approval by European Medicines Agency of an AAV gene therapy for lipoprotein lipase deficiency,[30,31] provide a solid rationale for planning the clinical testing of AAV gene therapy for other diseases with unmet clinical needs such as recessive CPVT.

Acknowledgments

We thank Patrizia Vaghi and Centro Grandi Strumenti of the University of Pavia for technical assistance in the confocal microscopy facility.

Sources of Funding

We acknowledge the support of the following research grants: Telethon grant GGP11141 (to Dr Priori), Telethon grant GGP08153 (to Dr Protasi), Foundation Leducq Research grant 0812 CVD 01 (to Dr Priori), We acknowledge funding for the Ricerca Corrente from the Minister of Health to support research infrastructures at the Maugeri Foundation.

Disclosures

None.

References

1. Coumel P, Maison-Blanche P, Catuli D. Heart rate and heart rate variability in normal young adults. *J Cardiovasc Electrophysiol*. 1994;5:899–911.
2. Priori SG, Napolitano C, Tiso N, Memmi M, Vignati G, Bloise R, Sorrentino V, Danieli GA. Mutations in the cardiac ryanodine receptor gene (*hRyR2*) underlie catecholaminergic polymorphic ventricular tachycardia. *Circulation*. 2001;103:196–200.
3. Lahat H, Pras E, Olender T, Avidan N, Ben-Asher E, Man O, Levy-Nissenbaum E, Khoury A, Lorber A, Goldman B, Lancet D, Eldar M. A missense mutation in a highly conserved region of CASQ2 is associated with autosomal recessive catecholamine-induced polymorphic ventricular tachycardia in Bedouin families from Israel. *Am J Hum Genet*. 2001;69:1378–1384.
4. Tester DJ, Arya P, Will M, Haglund CM, Farley AL, Makielski JC, Ackerman MJ. Genotypic heterogeneity and phenotypic mimicry among unrelated patients referred for catecholaminergic polymorphic ventricular tachycardia genetic testing. *Heart Rhythm*. 2006;3:800–805.
5. Nyegaard M, Overgaard MT, Søndergaard MT, Vranas M, Behr ER, Hildebrandt LL, Lund J, Hedley PL, Camm AJ, Wettrell G, Fosdal I, Christiansen M, Børglum AD. Mutations in calmodulin cause ventricular tachycardia and sudden cardiac death. *Am J Hum Genet*. 2012;91:703–712.
6. Roux-Buisson N, Cacheux M, Fourest-Lieuvin A, Fauconnier J, Brocard J, Denjoy I, Durand P, Guicheney P, Kyndt F, Leenhardt A, Le Marec H, Lucet V, Mabo P, Probst V, Monnier N, Ray PF, Santoni E, Trémeaux P, Lacampagne A, Fauré J, Lunardi J, Marty I. Absence of triadin, a protein of the calcium release complex, is responsible for cardiac arrhythmia with sudden death in human. *Hum Mol Genet*. 2012;21:2759–2767.
7. Cerrone M, Colombi B, Santoro M, di Barletta MR, Scelsi M, Villani L, Napolitano C, Priori SG. Bidirectional ventricular tachycardia and fibrillation elicited in a knock-in mouse model carrier of a mutation in the cardiac ryanodine receptor. *Circ Res*. 2005;96:e77–e82.
8. Cerrone M, Noujaim SF, Tolkacheva EG, Talkachou A, O'Connell R, Berenfeld O, Anumonwo J, Pandit SV, Vikstrom K, Napolitano C, Priori SG, Jalife J. Arrhythmogenic mechanisms in a mouse model of catecholaminergic polymorphic ventricular tachycardia. *Circ Res*. 2007;101:1039–1048.
9. Raffaele di Barletta M, Viatchenko-Karpinski S, Nori A, Memmi M, Terentyev D, Turcato F, Valle G, Rizzi N, Napolitano C, Gyorke S, Volpe P, Priori SG. Clinical phenotype and functional characterization of casq2 mutations associated with catecholaminergic polymorphic ventricular tachycardia. *Circulation*. 2006;114:1012–1019.
10. Rizzi N, Liu N, Napolitano C, Nori A, Turcato F, Colombi B, Bicciato S, Arcelli D, Spedito A, Scelsi M, Villani L, Esposito G, Boncompagni S,

Protasi F, Volpe P, Priori SG. Unexpected structural and functional consequences of the R33Q homozygous mutation in cardiac calsequestrin: a complex arrhythmogenic cascade in a knock in mouse model. *Circ Res*. 2008;103:298–306.
11. Paavola J, Viitasalo M, Laitinen-Forsblom PJ, Pasternack M, Swan H, Tikkanen I, Toivonen L, Kontula K, Laine M. Mutant ryanodine receptors in catecholaminergic polymorphic ventricular tachycardia generate delayed afterdepolarizations due to increased propensity to Ca^{2+} waves. *Eur Heart J*. 2007;28:1135–1142.
12. Hayashi M, Denjoy I, Extramiana F, Maltret A, Buisson NR, Lupoglazoff JM, Klug D, Hayashi M, Takatsuki S, Villain E, Kamblock J, Messali A, Guicheney P, Lunardi J, Leenhardt A. Incidence and risk factors of arrhythmic events in catecholaminergic polymorphic ventricular tachycardia. *Circulation*. 2009;119:2426–2434.
13. Priori SG, Napolitano C, Memmi M, Colombi B, Drago F, Gasparini M, DeSimone L, Coltorti F, Bloise R, Keegan R, Cruz Filho FE, Vignati G, Benatar A, DeLogu A. Clinical and molecular characterization of patients with catecholaminergic polymorphic ventricular tachycardia. *Circulation*. 2002;106:69–74.
14. Watanabe H, Chopra N, Laver D, Hwang HS, Davies SS, Roach DE, Duff HJ, Roden DM, Wilde AA, Knollmann BC. Flecainide prevents catecholaminergic polymorphic ventricular tachycardia in mice and humans. *Nat Med*. 2009;15:380–383.
15. Liu N, Denegri M, Ruan Y, Avelino-Cruz JE, Perissi A, Negri S, Napolitano C, Coetzee WA, Boyden PA, Priori SG. Short communication: flecainide exerts an antiarrhythmic effect in a mouse model of catecholaminergic polymorphic ventricular tachycardia by increasing the threshold for triggered activity. *Circ Res*. 2011;109:291–295.
16. Priori SG, Wilde AA, Horie M, Cho Y, Behr ER, Berul C, Blom N, Brugada J, Chiang CE, Huikuri H, Kannankeril P, Krahn A, Leenhardt A, Moss A, Schwartz PJ, Shimizu W, Tomaselli G, Tracy C. Executive summary: HRS/EHRA/APHRS expert consensus statement on the diagnosis and management of patients with inherited primary arrhythmia syndromes. *Heart Rhythm*. 2013;10:e85–108.
17. Atallah J, Erickson CC, Cecchin F, Dubin AM, Law IH, Cohen MI, Lapage MJ, Cannon BC, Chun TU, Freedenberg V, Gierdalski M, Berul CI; Pediatric and Congenital Electrophysiology Society (PACES). Multiinstitutional study of implantable defibrillator lead performance in children and young adults: results of the Pediatric Lead Extractability and Survival Evaluation (PLEASE) study. *Circulation*. 2013;127:2393–2402.
18. Denegri M, Avelino-Cruz JE, Boncompagni S, De Simone SA, Auricchio A, Villani L, Volpe P, Protasi F, Napolitano C, Priori SG. Viral gene transfer rescues arrhythmogenic phenotype and ultrastructural abnormalities in adult calsequestrin-null mice with inherited arrhythmias. *Circ Res*. 2012;110:663–668.
19. Crawley MJ. *The R Book*. Chichester, UK; Wiley; 2007.
20. White JD, Thesier DM, Swain JB, Katz MG, Tomasulo C, Henderson A, Wang L, Yarnall C, Fargnoli A, Sumaroka M, Isidro A, Petrov M, Holt D, Nolen-Walston R, Koch WJ, Stedman HH, Rabinowitz J, Bridges CR. Myocardial gene delivery using molecular cardiac surgery with recombinant adeno-associated virus vectors in vivo. *Gene Ther*. 2011;18:546–552.
21. Pacak CA, Mah CS, Thattaliyath BD, Conlon TJ, Lewis MA, Cloutier DE, Zolotukhin I, Tarantal AF, Byrne BJ. Recombinant adeno-associated virus serotype 9 leads to preferential cardiac transduction in vivo. *Circ Res*. 2006;99:e3–e9.
22. Vandendriessche T, Thorrez L, Acosta-Sanchez A, Petrus I, Wang L, Ma L, DE Waele L, Iwasaki Y, Gillijns V, Wilson JM, Collen D, Chuah MK. Efficacy and safety of adeno-associated viral vectors based on serotype 8 and 9 vs. lentiviral vectors for hemophilia B gene therapy. *J Thromb Haemost*. 2007;5:16–24.
23. Liu N, Denegri M, Dun W, Boncompagni S, Lodola F, Protasi F, Napolitano C, Boyden PA, Priori SG. Abnormal propagation of calcium waves and ultrastructural remodeling in recessive catecholaminergic polymorphic ventricular tachycardia. *Circ Res*. 2013;113:142–152.
24. Priori SG, Chen SR. Inherited dysfunction of sarcoplasmic reticulum Ca^{2+} handling and arrhythmogenesis. *Circ Res*. 2011;108:871–883.
25. Lehnart SE, Mongillo M, Bellinger A, Lindegger N, Chen BX, Hsueh W, Reiken S, Wronska A, Drew LJ, Ward CW, Lederer WJ, Kass RS, Morley G, Marks AR. Leaky Ca^{2+} release channel/ryanodine receptor 2 causes seizures and sudden cardiac death in mice. *J Clin Invest*. 2008;118:2230–2245.
26. Valle G, Galla D, Nori A, Priori SG, Gyorke S, de Filippis V, Volpe P. Catecholaminergic polymorphic ventricular tachycardia-related mutations R33Q and L167H alter calcium sensitivity of human cardiac calsequestrin. *Biochem J*. 2008;413:291–303.
27. Kim E, Youn B, Kemper L, Campbell C, Milting H, Varsanyi M, Kang C. Characterization of human cardiac calsequestrin and its deleterious mutants. *J Mol Biol*. 2007;373:1047–1057.
28. Xie Y, Sato D, Garfinkel A, Qu Z, Weiss JN. So little source, so much sink: requirements for afterdepolarizations to propagate in tissue. *Biophys J*. 2010;99:1408–1415.
29. Zsebo K, Yaroshinsky A, Rudy JJ, Wagner K, Greenberg B, Jessup M, Hajjar RJ. Long-term effects of AAV1/SERCA2a gene transfer in patients with severe heart failure: analysis of recurrent cardiovascular events and mortality. *Circ Res*. 2014;114:101–108.
30. Ylä-Herttuala S. Endgame: glybera finally recommended for approval as the first gene therapy drug in the European union. *Mol Ther*. 2012;20:1831–1832.
31. Ylä-Herttuala S. The need for increased clarity and transparency in the regulatory pathway for gene medicines in the European Union. *Mol Ther*. 2012;20:471–472.

CLINICAL PERSPECTIVE

Homozygous mutations in the *CASQ2* gene encoding for human calsequestrin-2, a protein that regulates calcium homeostasis, cause the recessive variant of catecholaminergic polymorphic ventricular tachycardia (CPVT). CPVT predisposes the hearts of patients to cardiac arrest elicited by stress and emotion. CPVT patients receive lifelong therapy with β-blockers to prevent cardiac arrest. Development of "curative" strategies to restore normal gene function is an attractive goal for the treatment of CPVT: a highly penetrant, life-threatening disease. In 2008, we developed and characterized a knock-in mouse model that recapitulates the human phenotype of recessive CPVT and harbors the R33Q mutation in the *CASQ2* gene. Here, we explore the therapeutic potential of viral gene transfer of wild-type *CASQ2* in R33Q mice using an adeno-associated virus serotype 9 (AAV9). In vivo delivery of the AAV9-*CASQ2* to R33Q mice prevents the development of the CPVT phenotype when therapy is administered to newborn R33Q mice and reverts the manifestations of the disease when administered to adult R33Q mice with full-blown signs of the disease. In the R33Q CPVT mice model, our gene therapy strategy shows long-term efficacy and selective expression of the transgene in the heart. The present data provide the first demonstration that delivery of the wild-type *CASQ2* gene is able not only to prevent the onset of disease but also to revert its multifaceted manifestations, including abnormal protein expression, altered architecture of junctional sarcoplasmic reticulum, and cardiac arrhythmias. These preclinical data provide the rational for envisioning viral gene transfer as a novel therapeutic approach in CPVT patients.

Single Delivery of an Adeno-Associated Viral Construct to Transfer the *CASQ2* Gene to Knock-In Mice Affected by Catecholaminergic Polymorphic Ventricular Tachycardia Is Able to Cure the Disease From Birth to Advanced Age

Marco Denegri, Rossana Bongianino, Francesco Lodola, Simona Boncompagni, Verónica C. De Giusti, José E. Avelino-Cruz, Nian Liu, Simone Persampieri, Antonio Curcio, Francesca Esposito, Laura Pietrangelo, Isabelle Marty, Laura Villani, Alejandro Moyaho, Paola Baiardi, Alberto Auricchio, Feliciano Protasi, Carlo Napolitano and Silvia G. Priori

Circulation. 2014;129:2673-2681; originally published online June 2, 2014;
doi: 10.1161/CIRCULATIONAHA.113.006901
Circulation is published by the American Heart Association, 7272 Greenville Avenue, Dallas, TX 75231

Print ISSN: 0009-7322. Online ISSN: 1524-4539

SUPPLEMENTAL MATERIAL

Supplemental Methods

In vivo pharmacological challenge

In vivo ECG recordings were performed using subcutaneous devices (Data Sciences International). Baseline ECGs were recorded for 30 minutes followed by intraperitoneal Epinephrine injection (2 mg/Kg) and an additional 30 minutes of continuous recording. All the animals were studied according to the protocols approved by the Animal Care and Use committee at the Maugeri Foundation, Pavia.

Immunohistochemistry

Hearts were collected and processed for paraffin embedding. Immunohystochemical analysis was performed with an anti-GFP antibody (1:30, Santa Cruz, SC-9996) and anti-mouse HRP conjugated secondary antibody (1:200, Promega). Sections were then revealed by peroxidase-diaminobenzidine (DAB) reaction for 2 min and counterstaining in according with standard procedures and analysed by bright-field light microscopy.

Isolation of Adult Mice Ventricular Myocytes

Ventricular myocytes were isolated using an established enzymatic digestion protocol[1] from wild type, R33Q, R33Q-INF and R33Q-GFP mice with the AAV9-CASQ2 construct of either sex at different ages.

Action potential recordings in Isolated Ventricular Myocytes

Isolated ventricular myocytes were seeded on a glass bottom perfusion chamber

mounted on the stage of an inverted microscope. After 5 minutes, the myocytes were bathed in the following solution at 35°C (in mmol/L): 140 NaCl, 4 KCl, 2 $CaCl_2$, 1 $MgCl_2$, 10 HEPES, and 5 Glucose, pH 7.4, with NaOH.

Action potential recording was performed using patch electrodes made of borosilicated (resistance of 2 to 3 MΩ) and filled with a solution containing (in mmol/L): 120 potassium aspartate, 20 KCl, 1 $MgCl_2$, 4 Na_2ATP, 0.1 GTP, 10 HEPES, 10 Glucose, pH 7.2, with NaOH. Signals were acquired at 10 kHz (Digidata 1322A, Axon Instruments) and analyzed with pCLAMP version 9.2 software (Axon Instruments). Quiescent, calcium-tolerant, rod-shaped cells with clear cross striations and a resting potential < –80 mV were electrically stimulated using depolarizing pulses with duration of 3 ms and amplitude of 1.5 fold the minimal current needed to evoke an action potential. Correction for the liquid junction potential between pipette and bath solution was performed.

Reverse-Transcription Polymerase Chain Reaction (RT-PCR) and Quantitative Real Time PCR

Total RNA was extracted and purified from isolated myocytes, liver, lung, skeletal muscle, spleen, kidney, testis and ovary of AAV9-*CASQ2* infected R33Q and R33Q mice. Real Time PCR quantification of mRNA of the target genes were processed by Bio-Rad CFX Manager software package (Bio-Rad Laboratories, Inc., USA) as previously described[1]. The following primers were used: *GFP*: Forward: 5'-CTATATCATGGCCGACAAGCAG-3' and Reverse: 5'-GCTCGTCCATGCCGAGAGTG-3'; *GAPDH*: Forward: 5'-GAAAGCTGTGGCGTGATG-3' and Reverse: 5'-GCCCAAGATGCCCTTCAGTG-3';

endogenous *CASQ2* (amplifying 5' UTR region): Forward: 5'-CCATGATCTCTATTCTGGAGACTG-3' and Reverse: 5'-ATGAAGAGGATTTACCTGCTCATG -3'; total *CASQ2* (amplifying exon 1): Forward: 5'-ATGAAGAGGATTTACCTGCTCATG-3' and Reverse 5'-GCTCCAGTACAATCTCCTTCAGC-3'. The mean values were normalized against the GAPDH. Values for Fold Expression were based on 2^-ΔΔCt methods.

SDS-PAGE and Western blotting

Animals were euthanized by cervical dislocation. Hearts were dissected and rapidly frozen in liquid nitrogen and then lysed with 1 ml of RIPA buffer (Thermo Scientific) with protease inhibitor cocktail (Sigma-Aldrich). The samples were quantified (BCA protein assay kit, Pierce, Thermo Scientific, Rockford, IL, USA) and 30 µg of total protein were loaded on a 4-12% linear gradient polyacrylamide gel (Invitrogen) and run at 200 mV for 1 hour at room temperature. The proteins were transferred to a nitrocellulose membrane (Invitrogen) at 30 mV for 2 hours at 4ºC. Non-specific binding was blocked with 3% non-fat dry milk (Sigma-Aldrich) in TBS-T (Sigma-Aldrich). The membrane was then incubated for 1 hour at room temperature with primary antibody: anti-CASQ2 (ABR, PA1-913), anti-Triadin[2], anti-Junctin[1], anti-RyR2 (ABR, MA3-916), anti-α-Actinin (Sigma-Aldrich, A7811), anti-Cadherin (Sigma-Aldrich, C1821) and anti-Actin (Sigma-Aldrich, A1978). The blot was incubated with HRP-conjugated anti-rabbit/anti-mouse antibody (Promega, 1:3500). The detection was performed with the Supersignal West Pico Chemiluminescent substrate (Pierce) and exposed using X-ray film (KodaK).

ImmunoFluorescence

Indirect immunofluorescence labeling was performed on ventricular cardiac myocytes isolated from R33Q-INF mice. The samples were blocked with 10% Donkey serum (Sigma-Aldrich) for 1 hour, followed by incubation with primary antibodies anti-CASQ2 (PA1-913; ABR), anti-α-Actinin (Sigma-Aldrich, A7811) and anti-RyR2 (ABR, MA3- 916). Secondary antibodies were Alexa Fluor 405 goat anti-mouse and Alexa Fluor 546 goat anti-rabbit IgG. The coverslips were mounted using Dako fluorescent mounting medium (Dako). Confocal microscopy was performed with a Leica TCS-SP5 digital scanning confocal microscope equipped with a HCX PL APO 40x/numerical aperture =1.25 oil immersion objective. We used the He/Ne laser line at 580-630 nm. The pinhole diameter was kept at Airy 1. Images were exported to Adobe Photoshop (Adobe Systems, Mountain View, CA).

Electron Microscopy

Hearts isolated from WT, R33Q, R33Q-INF and R33Q-GFP mice were fixed by retrograde aortic perfusion with 3.5% glutaraldehyde in 0.1 mol/L NaCaCo buffer (pH 7.2) and analyzed. Small bundles of cells were post-fixed in 2% OsO_4 in NaCaCo buffer for 2 hours and then block-stained in saturated uranyl acetate. After dehydration, specimens were embedded in an epoxy resin (Epon 812). Ultrathin sections were cut in a Leica Ultracut R microtome (Leica Microsystem, Austria) using a Diatome diamond knife (Diatome Ltd. CH-2501 Biel, Switzerland) and double stained with uranyl acetate and lead citrate. All sections were examined with an FP 505 Morgagni Series 268D electron microscope (FEI Company, Brno, Czech Republic), equipped with Megaview III digital camera. The average width of jSR terminal cisternae was measured in random images (more than 100 images) at 56.000X using the Soft Imaging System.

Supplemental Figures and Supplemental Figure Legends

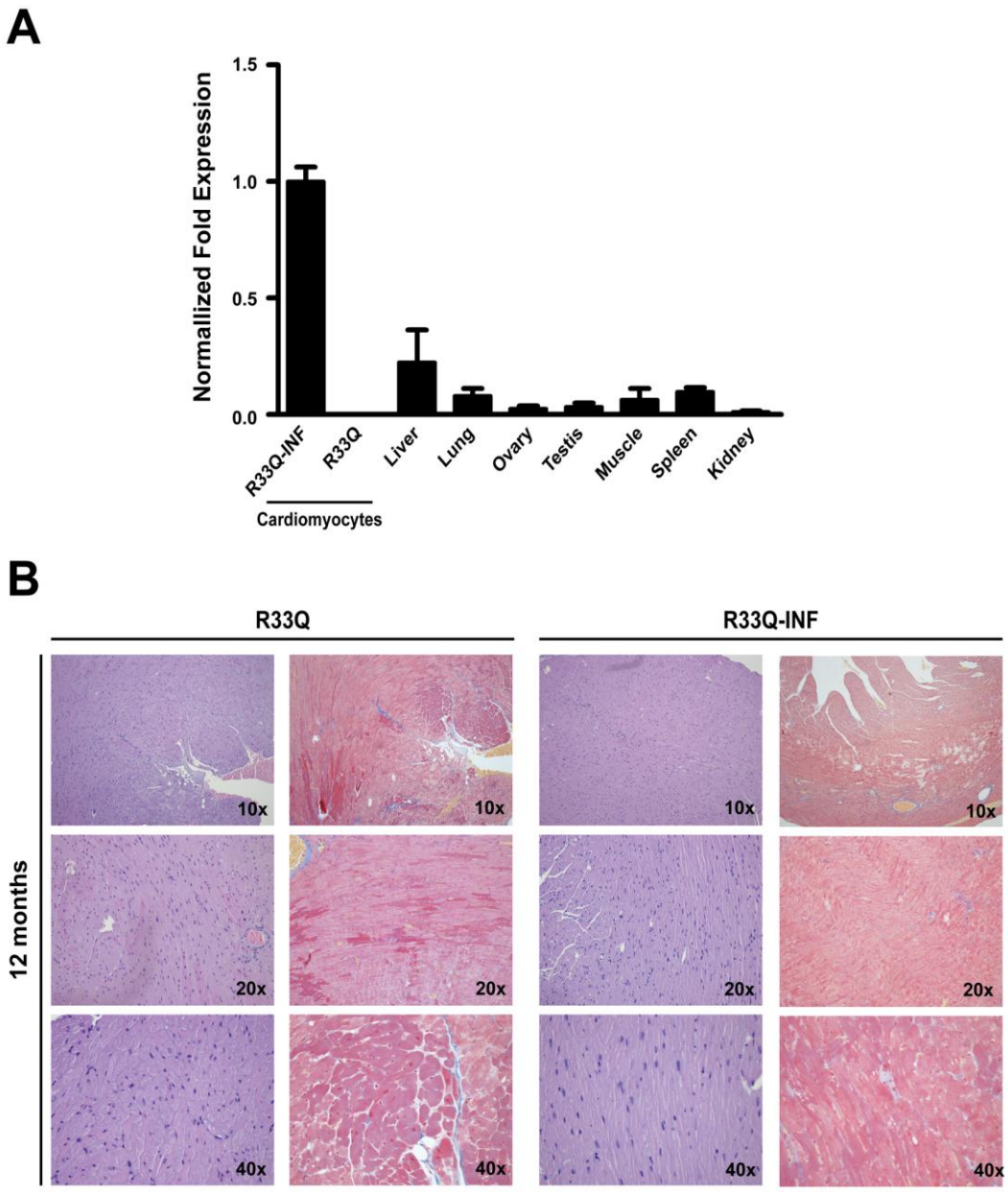

Supplemental Figure 1: Long term Adeno-Associated viral infection distribution in AAV9-*CASQ2* infected newborn R33Q mice.

A, Real-time polymerase chain reaction quantification of *GFP* expression in R33Q cells and AAV9-*CASQ2* infected R33Q (R33Q-INF) cells and organs (n= 3 mice at 12 months post infection). B, Different magnification (10x, 20x and 40x) of hematoxylin-eosin (left) and Masson's trichrome (right) stainings in R33Q and R33Q-INF hearts 12 months post infection (n= 2 mice/each condition).

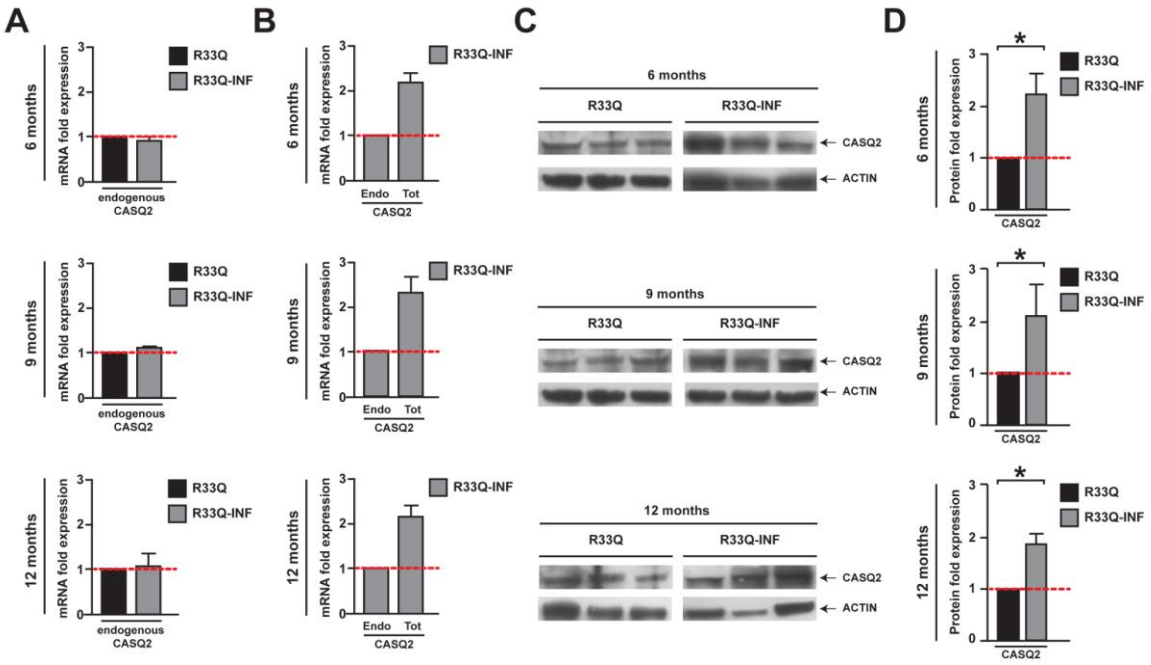

Supplemental Figure 2: Analysis of mRNA and protein expression in AAV9-*CASQ2* infected newborn R33Q mice.

A, quantification of endogenous *CASQ2*-mRNA obtained by Real-Time PCR amplifying a portion in 5' UTR of the transcript in R33Q and AAV9-*CASQ2* infected R33Q mice (R33Q-INF) in all age groups. B, quantification of total vs endogenous *CASQ2*-mRNA in R33Q-INF mice, obtained by Real-Time PCR amplifying exon 1 of the coding sequence (Tot) and a portion in 5' UTR of the transcript (Endo), respectively, in 6, 9, 12 months old mice infected at birth. C, analysis of CASQ2 protein in heart derived from R33Q and R33Q-INF mice. Actin was used as a loading control. D, protein quantification of CASQ2 expression in R33Q-INF normalized on R33Q mice ± Standard Deviation (*p<0.05, R33Q-INF vs R33Q).

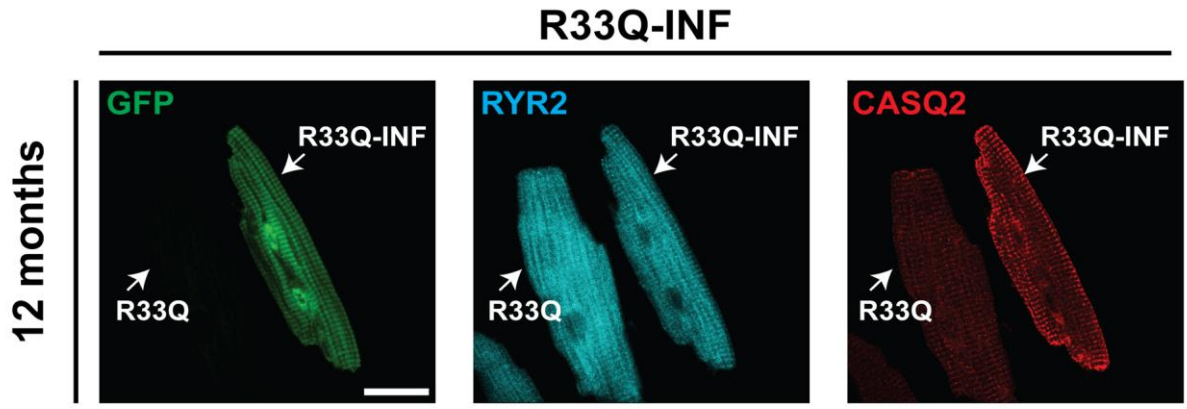

Supplemental Figure 3: Long term protein expression and distribution analysis of the virally induced CASQ2 in infected newborn R33Q mice.

Comparison of protein expression of CASQ2 and RyR2 in an infected (GFP positive, R33Q-INF) and not infected (GFP negative, R33Q) myocytes isolated from AAV9-*CASQ2* infected newborn R33Q (R33Q-INF) mouse 12 months post viral delivery. No differences in the fluorescence intensity of the staining with anti-RyR2 antibody are detected while it is possible to appreciate, on equal terms of acquisition, a higher CASQ2 fluorescence intensity in R33Q-INF vs R33Q. Scale bar = 20 μm.

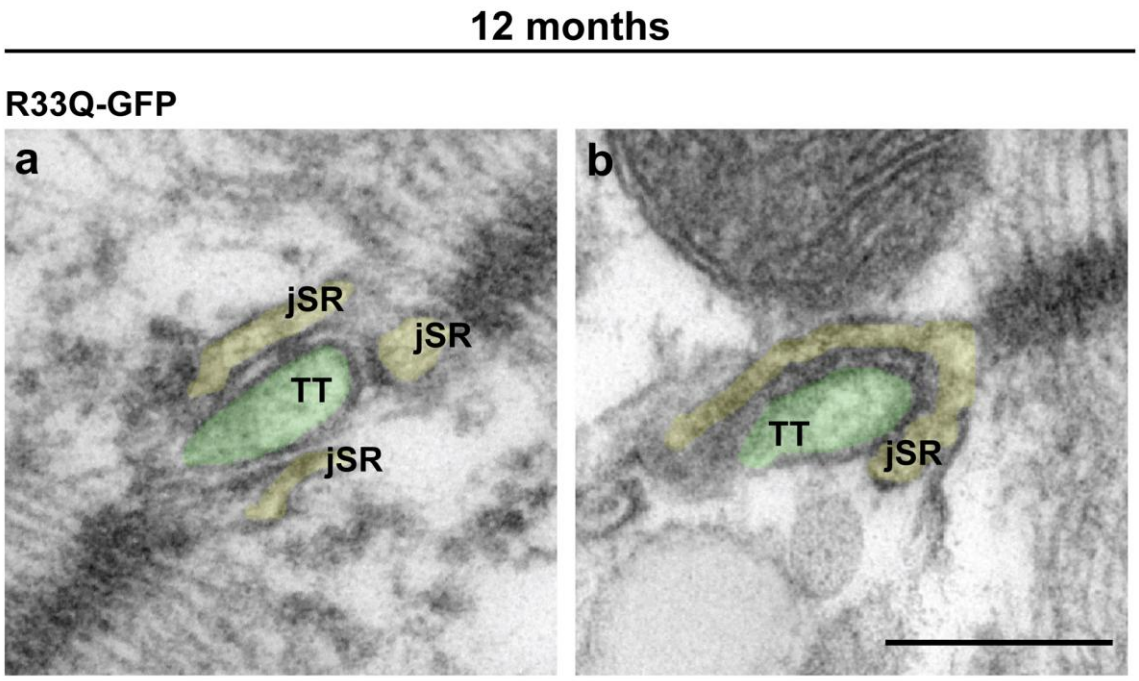

Supplemental Figure 4: Ultrastructural analysis of CRUs in 12 months-old R33Q mice infected with AAV9-*GFP* at birth.

Electron micrographs of CRUs of AAV9-*GFP* infected newborn R33Q (R33Q-GFP: a, b) hearts at 12 months post infection (n= 3 mice). Transverse-tubules (TT) are labelled in green, while junctional Sarcoplasmic Reticulum (jSR) is in yellow. Scale bar = 0.1 µm.

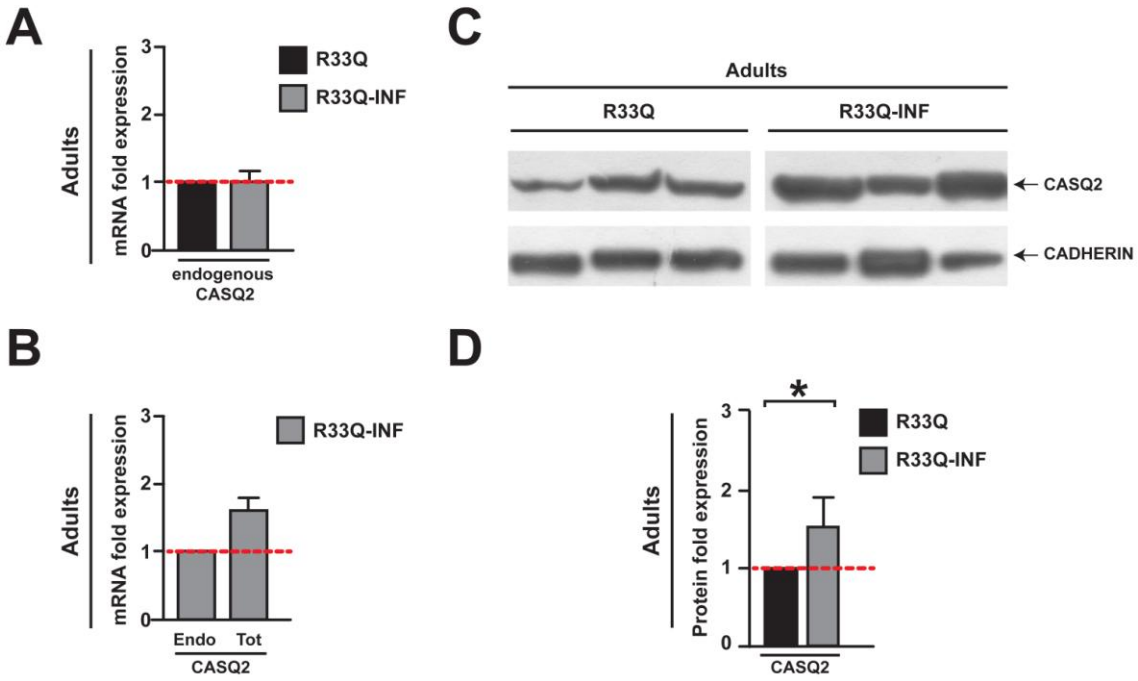

Supplemental Figure 5: Analysis of mRNA and protein expression in AAV9-*CASQ2* adult infected R33Q mice.

A, quantification of endogenous *CASQ2*-mRNA obtained by Real-Time PCR amplifying a portion in 5' UTR of the transcript in R33Q and AAV9-*CASQ2* infected R33Q (R33Q-INF) adult mice. B, quantification of total vs endogenous *CASQ2*-mRNA in R33Q-INF mice, obtained by Real-Time PCR amplifying exon 1 of the coding sequence (Tot) and a portion in 5' UTR of the transcript (Endo), respectively, in age grouped and adult mice. C, analysis of CASQ2 protein in heart derived from R33Q and R33Q-INF adult mice. Cadherin was used as a loading control. D, protein quantification of CASQ2 expression in adult R33Q-INF normalized on R33Q mice ± Standard Deviation (*p<0.05, R33Q-INF vs R33Q).

Supplemental Reference

1. Denegri M, Avelino-Cruz JE, Boncompagni S, De Simone SA, Auricchio A, Villani L, Volpe P, Protasi F, Napolitano C, Priori SG. Viral gene transfer rescues arrhythmogenic phenotype and ultrastructural abnormalities in adult calsequestrin-null mice with inherited arrhythmias. *Circ Res*. 2012;110:663-668

2. Roux-Buisson N, Cacheux M, Fourest-Lieuvin A, Fauconnier J, Brocard J, Denjoy I, Durand P, Guicheney P, Kyndt F, Leenhardt A, Le Marec H, Lucet V, Mabo P, Probst V, Monnier N, Ray PF, Santoni E, Trémeaux P, Lacampagne A, Fauré J, Lunardi J, Marty I. Absence of triadin, a protein of the calcium release complex, is responsible for cardiac arrhythmia with sudden death in human. *Hum Mol Genet*. 2012;21:2759-2767